Physics and Evolution of HEMP-Thrusters

IEPC-2007-108

Presented at the 30th International Electric Propulsion Conference, Florence, Italy
September 17-20, 2007

Günter Kornfeld*, Norbert Koch.†, Hans-Peter Harmann‡

Thales Electron Devices GmbH, Söflingerstr. 100, 89077 Ulm, Germany

Abstract

Nine years after the first patent and 7 years after the start of hardware development, the physical properties and functioning principles of the HEMP-thruster (Highly Efficient Multistage Plasma Thruster, HEMP-T) concept are well understood only in a small group of people directly involved in the development programs of this new, promising thruster concept. This paper therefore tries to close an informational gap within the Electric Propulsion (EP) community and to foster the understanding of the HEMP-T as an own class of ion thrusters besides Grid Ion Thrusters (GITs) and Hall Effect Thrusters (HETs). This might be especially useful at a time where HEMP-Ts observe interest from spacecraft designers[1,2], mission engineers and satellite operators, caused by the HEMP-Ts operational characteristics allowing reliable, low cost and low complexity EP systems.

Though being a grid less device, the HEMP-T shows like a GIT a clear separation of ionization and ion acceleration zones. Therefore, performance similarities with GITs as e.g. high specific impulse (>3000 s) and high beam power efficiency (>80%) are found. Otherwise the HEMP-T is clearly a magnetic device. With **ExB** areas in the cusp zones it shows similarities to HETs. But unlike HETs, the unique cusp/mirror magnetic field topology, created by a Permanent Periodic Magnet (PPM) stack, confines the discharge plasma off the dielectric thruster channel walls and is reason for the channel erosion free operation. A detailed comparison will be presented between GIT, HET and HEMP-T, based on their respective physical properties.

A power balance model of the HEMP-T is provided, showing good agreement to the observed thermal losses and their locations at thruster anode and magnetic cusp zones. The model explains the advantages of the multistage compared to a single cusp thruster concept.

Nomenclature and Abbreviations

EIT	=	electron ionization thruster (Kauffmann type thruster)
EP	=	electric propulsion
DLR	=	German aerospace flight center
ESA	=	European space agency
FCU	=	flow control unit
GIT	=	grid ion thruster
HEMP-T	=	high efficiency multistage plasma thruster
HET	=	Hall effect thruster
PPM system	=	permanent periodic magnet system
PSCU	=	power supply and control unit
RIT	=	radio frequency ionisation thruster
RF	=	radio frequency
SGEO	=	small GEO satellite; ESA ARTES 11 communication satellite
TWT	=	traveling wave tube

* Head of Business Development, guenter.kornfeld@thalesgroup.com.
† Head of EP R&D, norbert.koch@thalesgroup.com.
‡ Project Manager HEMP-T IOD,hans-peter.harmann@thalesgroup.com.

I. Origin and Evolution of the HEMP Thruster Concept

THE conceptional ideas of the HEMP-Thruster originate in the experience and daily work with Traveling Wave Tubes (TWTs) at Thales Electron Devices. Those TWTs are used for amplification of the downlink RF signal on Telecom Satellites. In those electron devices, the power of a several kV electron beam is used to amplify a RF signal from mW into 100 W level. As shown in the TWT cross section in the upper part of figure 1.1, the electron beam is generated in an electron gun, focused through the inner tunnel of a helical RF delay line where the RF amplification between the Rf input and Rf output takes place and finally collected as slowed down spent electron beam on several, typically 2 to 4, subsequently voltage depressed collector stages. To maintain the electron beam diameter throughout the helical Rf interaction zone, the radial space charge forces in the electron beam are counter acted by the magnetic field forces created by a PPM (Permanent Periodic Magnet) System. The part in middle of figure 1.1 shows in detail the PPM focusing effect on the electron beam. The lower part of figure 1.1 shows as an example a crosscut and the axial magnetic field of a magnetically focused 2 stage collector where the slow beam electrons are collected at a depressed voltage Uc1 and the fast electrons at a further depressed voltage Uc2 < Uc1. This arrangement reduces the kinetic energy of the landing electrons and thus improves the overall TWT efficiency.

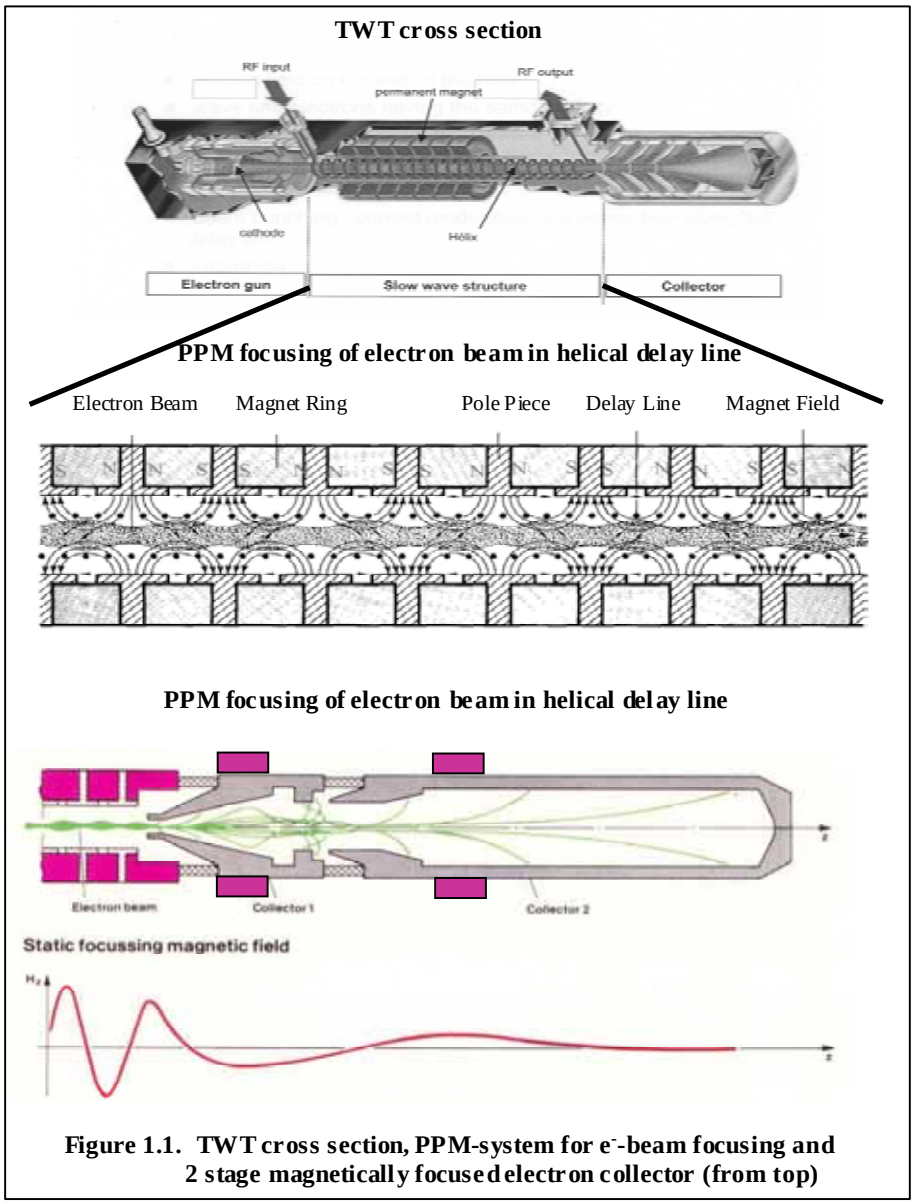

Figure 1.1. TWT cross section, PPM-system for e^--beam focusing and 2 stage magnetically focused electron collector (from top)

Several of those TWT conceptions were applied to the original HEMP-T concept:

The first basic idea in 1996 was to use for a thruster similar PPM field configurations as in a TWT to keep the plasma off the cylindrical walls of the discharge channel.

The second idea was to employ a multi stage plasma chamber. Like in a TWT collector, each magnetic cell should be operated at a subsequently depressed electrode potential in order to reduce kinetic energy losses of the plasma electrons to the anode.

The third thought was to insert a fast primary electron beam, generated by an electron gun, into a segmented discharge chamber. The electron beam was likewise intended to initiate the propellant ionization while traveling through the discharge chamber and also to neutralize after its deceleration at the thruster exit the ion beam.

Other TWT related background knowledge and a specific observation on a TWT with a micro leak supported strongly the feasibility of such a thruster concept as pointed out in the footnote.* Those ideas slowly emerged and found their condensation in a first patent in 1998 and are sketched in the upper part of Figure 1.2.

. The lower part of this figure shows the relatively complicated technical design of the first HEMP demonstration models DM1 and DM2 as they were manufactured within a DLR feasibility study in early 2001. The test results were not at all like they were expected: Though a discharge could be easily excited in the chamber, the major ion beam effect was not resulting in thrust but in erosion of the next downstream segment walls. Instead of measuring via the temperature increase of a thermal target the goal thrust value of 7 mN, with good will, a few µN could be attributed.

What was wrong?

1) When Xe was fed into the discharge chamber, the cathode emission was strongly poisoned and reduced in spite of pumping through the exhaust tube on the left side of the electron gun. Discharge current and primary electron current from the thermionic emitter could never be matched.
2) Strong discharging events outside the thruster in the vacuum tank occurred, which can be contributed to the lack of electrons downstream the thruster. Today we understand that even in case sufficient primaries would have been emitted, those decelerated electrons would have been mainly trapped inside the thruster at the magnetic exit cusp and could therefore not have been used to neutralize an exiting positively charged ion beam.
3) Though having independent voltage sources to apply the different potentials to the segmented electrodes, the intermediate downstream segment potentials adjusted themselves, due to their low impedance in the plasma discharge, within only 10 to 50 V lower than the anode.

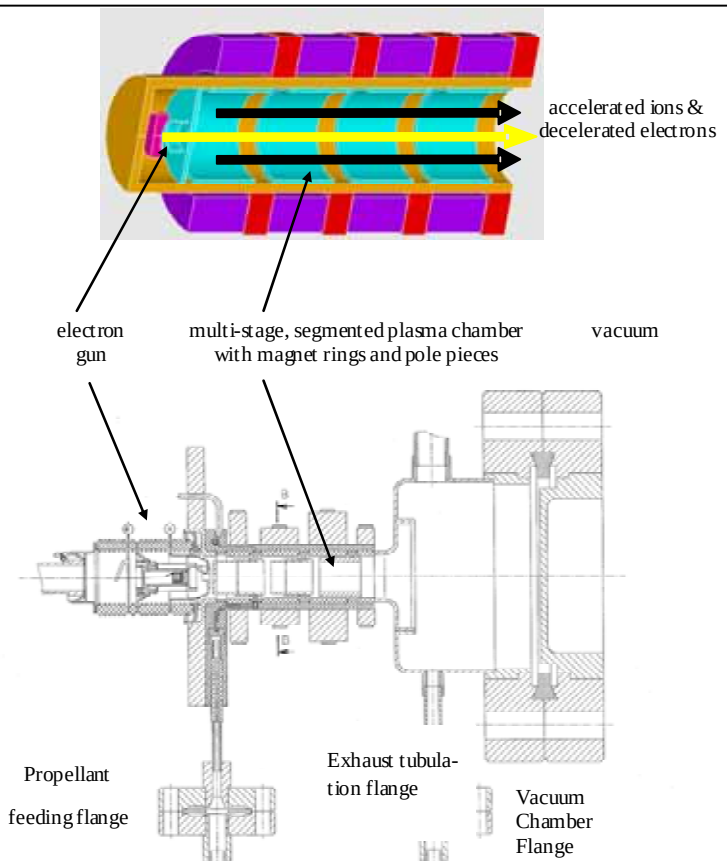

Figure 1.2 HEMP Thruster principle as patented in 1998 and first technical realisation in 2001 (lower part)

* An earlier observation on a defective, but still operational TWT supported the feasibility of a magnetically focused multistage plasma thruster: Due to a micro leak, the inside TWT pressure allowed to ignite a plasma along the electron beam volume. As is well known in such cases one can find an ion spot on the center of the cathode. In this case we also found an ion spot on the backside wall of the fourth collector stage of the magnetically focused collector with a potential close to cathode. This indicated that an ion beam had been formed, accelerated and focused to this spot, thus representing a sort of ion thruster in a magnetic and electrostatic multistage configuration.

After an intermediate but finally not successful trial to improve the results by using a newly designed electron gun which allowed lower residual pressures around the thermionic cathode, the following decisions were taken at the end of 2001:

a) Replacement of the electron gun on the upstream side of the thruster by a standard neutraliser downstream, as used in all standard ion thruster concepts.
b) Using the center anode hole as Xe propellant gas -, rather than as primary electron beam inlet into the discharge chamber.
c) Isolation of the ineffective segmented electrodes from the plasma by the insertion of a 0.5 mm thin walled, 9 mm inner diameter BN tube as new discharge channel wall.
d) Improvement of the fixture of the permanent magnet rings.

With those changes, a HEMP-T DM3 was assembled and first time tested in March 2002 on a thrust balance at the Onera facilities in Palaiseau, France. This test campaign and 2 following ones were supported besides the DLR, within the feasibility study, by the French CNES. The measured thrust of 1mN first time reached the order of magnitude where concept feasibility could be considered. On the other side the power efficiency was with approximately 10% still rather low. An explanation for that was found with the help of first plasma simulations.

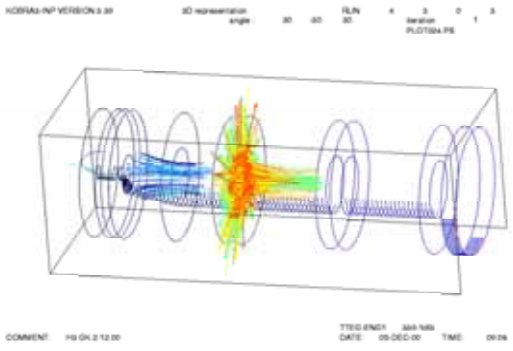

Figure 1.3. Simulation of electron trajectories in the HEMP-T DM 3

At that time and since 2000, our three people electric propulsion group performed also first plasma simulations in parallel to the hardware development. The codes used were not at all fully selfconsistantly. One was the KOBRA collissionless 3D trajectory code of Spädtke, the other the Berkeley XOOPIC particle in cell code. Nevertheless both codes, when applied to the special magnetic field pattern, suggested that the plasma electron confinement due to the mirror effect at the magnetic cusps was quite impacted and reduced by the low discharge channel diameter of only 9 mm, leading to high losses of kinetic energy at the discharge chamber walls in the cusp area as indicated by figure 1.3.

This led as next major improvement step to:

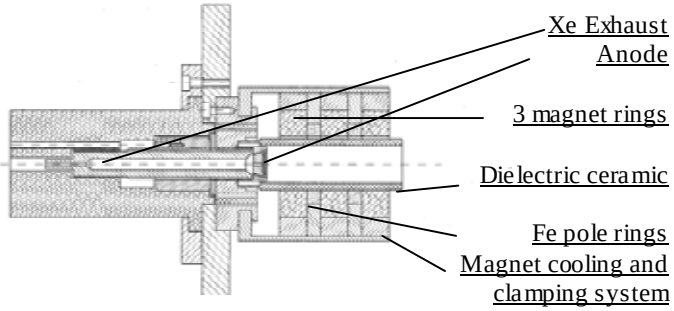

Figure 1.4. Cross section through HEMP-T DM3a

e) A discharge chamber diameter adapted with 14 mm already much better to the magnetic cusp field situation.

Three months after the DM3 test at Onera, the new hardware, called DM3a, could be tested again on the thrust balance of Onera. With 24 mN max thrust and a total efficiency up to about 30% a remarkable progress[3] could be demonstrated, underlining the potential of the new concept. An interesting feature of this early HEMP-T DM3a model (see figure 1.4.) was the conical hollow ion beam characteristic. Operating the thruster at 500 V anode voltage, Figure 1.5 shows the single charged Xe ion energy distribution for different polar angles. On the axis (0°), only a small amount of low energetic (50eV) ions were found, whereas the maximum peak with 500V ions occurred at 35° angle. The diagnostic tool used was an angular and energy selective mass spectrometry at IOM in Leipzig. The test was performed in October 2002. Another unusual feature there revealed was the relative high amount of double charged ions. It was found up to 20 % of the total ion beam with almost the same energy spectrum as the single charged ions (see figure 1.6).

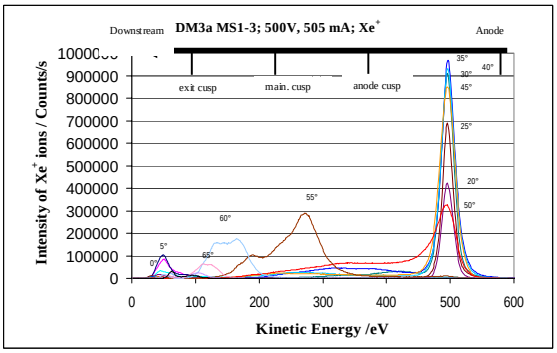

Figure 1.5. Energy Spectrum of single charged Xe ions for different polar angles

The intermediate energy peaks in special angular directions (e.g. at 280 V in 55° angle) were attributed to the different downstream ionization regions in the cusped thruster channel. Due to the work on the multicusp magnetic circuit those intermediate peaks and the related high divergence angles could be meanwhile much improved. The latest status in that respect is provided in two papers of the proceedings of this conference[4,5].

Since the recent HEMP-T development results will be covered in those papers we conclude our short historical review on the evolution of the HEMP thruster type with the steps leading to DM6 thruster. This could first time be called a HEMP-T 3050, for nominal 3000 s specific impulse and 50 mN thrust, respectively:

f) As the diameter increase worked out successfully in DM3a, the main cusp inner ceramic diameter was further increased to 20 mm.

g) To further reduce the plasma electron impact on the ceramic walls between the cusps, the contours of the magnetic field lines and the inner surface of the ceramic chamber were more paralleled by increasing the length of the exit magnet ring compared to the upstream magnets

h) In addition, throughout all the development phases a series of different magnet configurations and small geometrical modifications were analyzed by the commercial Maxwell 2 D code, interesting versions were then assembled and characterized in their thruster characteristics.

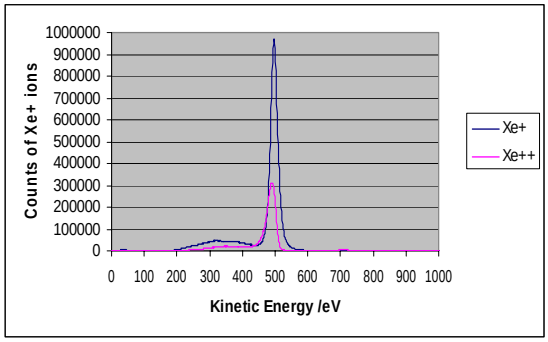

Figure 1.6. Energy Spectrum of single and double charged Xe ions at 35° angle

As a result, improved performances were obtained on a DM6 version of the HEMP thruster during a third test campaign at Onera in March 2003. Shortly after, they could be presented during the 28th IEPC in Toulouse[3]. Figure 1.7 shows these results. Whereas the total anode efficiency was with 37% still a little low. The evolution summary of the feasibility phase of the HEMP shows in figure 1.7 for DM6 impressive results for the thermal efficiency 78%, the 129 mN thrust and the 2679 s specific anode impulse. To get a comparison to the today's performances of our medium and high power HEMP-Ts, the data for the HEMP-T 3050 DM9.2 and the HEMP-T

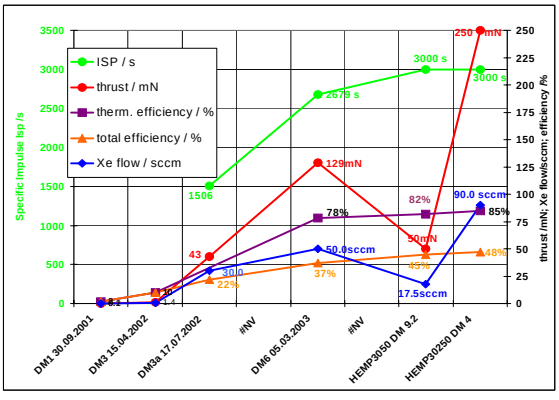

Figure 1.7. Evolution of the HEMP-T during the feasibility study and till mid 2007: ISP, thrust, thermal- and anode efficiency.

30250 DM4 are added in 2 columns I figure 1.7.

The very low thermal losses can directly be attributed to the low contact of the discharge plasma with the channel walls, which is a major characteristic of the new magnetic plasma confinement concept of the HEMP-T.

Figure 1.8 shows the DM6 thruster in operation, together with a first model of the new Thales neutraliser which is using a thermionic cathode insert based on a Ba/Ca- aluminates impregnated tungsten/osmium mixed metal matrix. The excellent performance characteristics of this neutraliser will be presented in a separate paper on this conference[6].

Figure 1.8 Historical view on HEMP-T DM 6 and Thales neutraliser

As an optical reference to the today's thruster design and operation, figure 1.9 shows a 50° side view on a DM9.1 and DM9.2 thruster cluster obtained under the ESA TRP "High power HEMP thruster module" program.

Figure 1.9. Two HEMP 3050 thrusters mounted on a horizontal bar in 40 cm distance on top of the thrust balance. Thruster s are operating on one anode supply line at 1000V, individual thruster adjustments by Xe flow to: 2x 2 kW, 2 kW + 300 W and 300 W+ 2 kW (from left to right)

II. Physical Properties of the HEMP Thruster in comparison to HETs and GITs

In this section we concentrate on the physical properties of the HEMP-Ts in comparison to HETs and GITs. This will increase the understanding of the concepts and their differences. To create a basis which can be referenced, figure 2.1 shows schematics of all three thruster types. We will see that the HEMP-T behaves in several aspects like a HET but in other aspects like a GIT. A group of aspects are quite unique to the HEMP-T. In the summary table 2.1 of this chapter, a column indicates whether the HEMP-T behaves in the respective aspect like a HET, like a GIT or is unique. The following sequence and numbering of the compared properties is maintained in table 2.1:

1) Axial electron impediment

HETs and HEMP-Ts impede the axial movement of the neutraliser electrons by crossed (radial) magnetic fields. For HETs the axial zone with significant radial B field typically extends over a distance of cm at the thruster exit, for the HEMP-Ts, the radial B field is axially concentrated over a few mm in the three magnetic cusps. Due to the much higher magnet fields there, the impeding effect is much higher, leading to a very low portion je0 of few % of electron current contributed from the neutraliser to the anode discharge current Ia,. For HETs this portion je0 is about 20% to 30%. The main plasma potential drop and thus accelerating E-fields occur across these radial B field zones leading to the typical **ExB** electron drift configuration (see figures 2.1).

In GITs the axial impediment of the neutraliser electrons is essentially completely done by the negatively polarized acceleration grid (see figure 2.1)

2) Ion beam power efficiency

Since the product Ua* je0 contributes directly to the thermal thruster losses at the anode or the thruster channel walls, the beam power efficiency of a HEMP-T (converting electric power into kinetic ion beam power) is much

higher (80% to 85%) than for a HET (60% to 70%) and similar to GITs. This may be a sufficient reason for naming the thruster high efficiency multistage plasma thruster.

3) Operation capability without neutraliser in a vacuum tank

Due to the high electron impedance of HEMPTs and GITs both can operate in a vacuum tank in principle without a neutraliser since the ion beams are neutralized at the grounded tank walls and no significant electron current is required to maintain the ionization in the discharge chamber, whereas HETs need additional neutraliser current to compensate for the electron energy losses at the discharge chamber walls and to sustain the discharge.

4) Plasma confinement in the thruster discharge chamber

For all thruster types, the ionization takes place in a dielectric discharge chamber. From energetic or efficiency point of view, the designers are normally aiming to reduce plasma losses to the walls to a minimum. For HEMP-Ts this goal is almost ideally reached by having the B-field mainly parallel to the channel walls. Only in the cusp region magnetic field lines are radially crossing the chamber walls. In those areas the strong radial magnetic field gradients are repelling the plasma from the walls. According to the well known magnetic mirror conditions and depending on the magnitude of the B-field at the considered position 1 and at the cusp field at the wall position c1 on the same field line, only electrons at position 1, with a velocity direction within the acceptance angle α_a, with respect to the magnetic B-field, $\alpha_a \le \arcsin\left(\sqrt{B1}/\sqrt{Bc1}\right)$, can reach the cusp at c1 (without considering further collisions). If an electron is started e.g. in an ionization process, we consider its angular velocity directions with respect to the flux direction as equally distributed. Therefore by integrating all angles from 0 to α_a, we get the relative probabilities pm for electrons able to reach the cusp at the wall. The figure 2.2 shows p1 for example as function of x, where x is the subject ratio x= Bm/Bcm, m is the mth cusp. Depending on the values of Bm and Bcm for the HEMP-T, these probabilities are only small fractions of ~ 5% to 10% of the electrons. We will later mention the values in table 3.1.

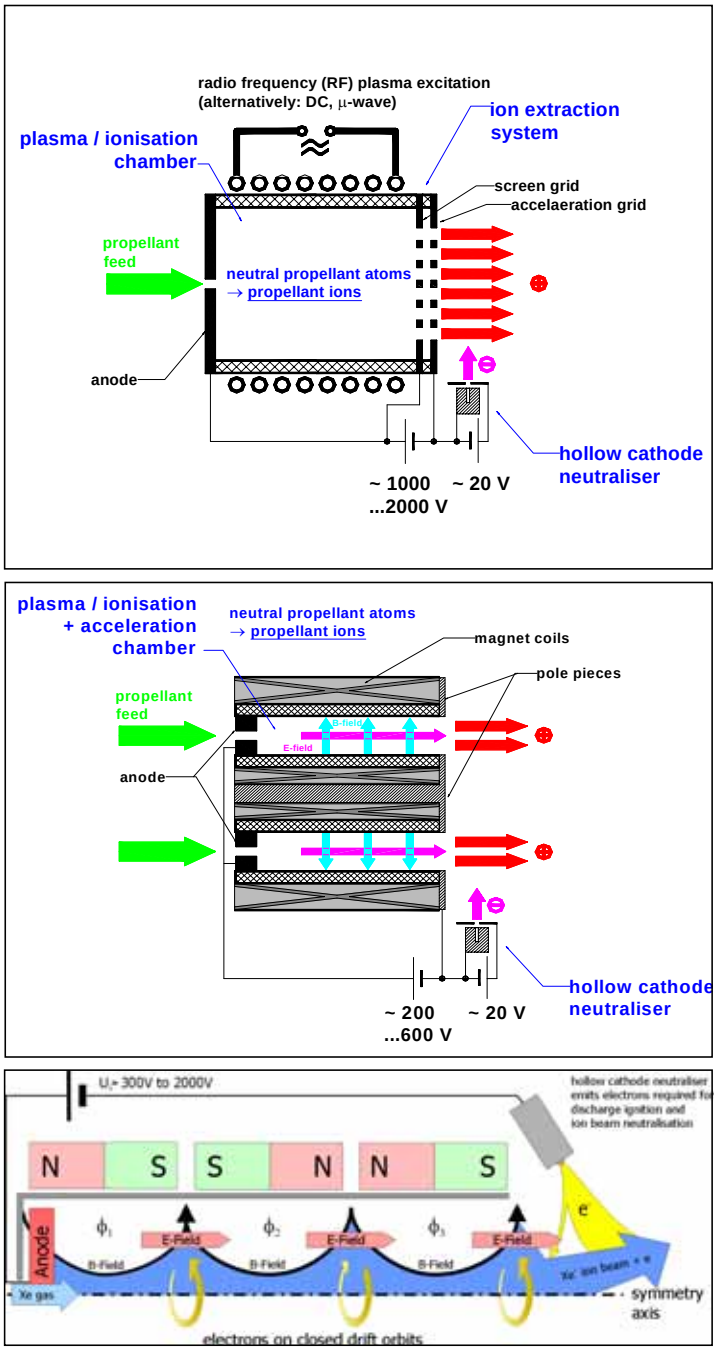

Figure2.1. Schematics of the 3 compared thruster types GIT (RIT), HET and HEMP-T (top down respectively)

For a HET this radial plasma confinement is only poor, even more, if it would be improved the thruster would have a problem to operate at all, because secondary electron emission at the walls is required to sustain sufficient

electron current for the ionization process. In other words, the radial magnetic field throughout the channel cross section would without wall contacts and secondary emission impede electrons too strongly to sustain the upstream ionization process.

For the GITs only the Kauffmann thrusters have a magnetic confinement in their discharge chamber, saving some plasma wall losses. RITs today have no magnetic plasma confinement at all in their ionization chamber.

5) Separation of ionization and acceleration zones

HEMP-T: Amongst the typically 3 cusps, the exit cusp has the strongest magnetic mirror parameters and due to the lower neutral gas density with lower collision frequency also the highest Hall parameter. Therefore the steepest potential drop occurs at the exit cusp. The few electrons being able to cross the exit cusp and entering close to the axis the upstream magnetic cell provide their gained kinetic energy within this cell to inelastic collision phenomena as ionization, excitation and elastic collisions resulting in a thermalisation of the plasma electrons within this extended magnetic cell with almost axiparallel magnetic field and constant plasma potential. As an effect we get an extended ionization zone on almost constant plasma potential out of which the ions are accelerated by a strong axial electric field (steep potential drop) across the exit cusp. We observe therefore a clear spatial separation of ionization and acceleration.

$$p1 := \frac{2\pi \left(\int_0^{\alpha 1} \sin(\theta)\, d\theta \right)}{4\pi}$$

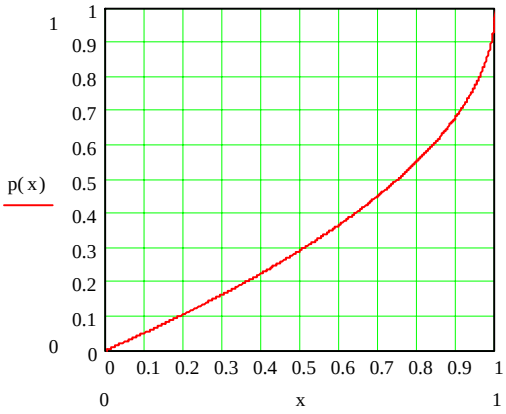

Figure 2.2. Probability of electrons to reach the cusp surface as function of the ratio x of axial field to cusp field.

HET: By design, the HET is lacking a median with axial magnetic field as electron port through which electrons can travel fast into a more upstream region where they can provide their kinetic energy to the statistical ionization processes. Due to the radial magnetic field throughout the channel cross section they need ionization and wall collisions, to proceed from their ExB drift movement to a more upstream axial position. By that, they loose continuously at each intermediate plasma potential value their kinetic energy and ionization and acceleration zones are intimately linked to each other.

GIT: Due to the negatively polarized acceleration grid no electrons, emitted from the neutraliser cathode, can enter the ionization discharge chamber. Ionization strictly takes place in the upstream discharge chamber either by electron bombardment between a main hollow cathode and the anode potential or in case of RITs by a ionization due to RF power injection. Acceleration on the other side occurs dominantly between the screen grid on anode potential and the negatively polarized acceleration grid. The lack of electrons in this intermediate region is the cause why the ion emission is space charge limited, requesting comparatively large diameters for a certain ion current.

6) Specific Impulse (Isp)

The specific impulse is defined as $Isp = \frac{T}{\dot{m} \cdot g} = \frac{v}{g}$, where T is the thrust, $\dot{m}$ the propellant mass flow, v the average exit velocity of all originally injected propellant particles leaving the thruster (that includes also not ionized neutral particles)and g.= 9.81m/s² the earth acceleration constant. Assuming that all particles would be single stage ionized (which is in a grid ion engine in a good approximation the case) then the velocity v is given by

$v = \sqrt{2\frac{q \cdot U}{M}}$, where q is the particle charge and M the mass. We see that velocity and specific impulse should be adjustable, they increase with the square root of the applied anode voltage.

For GITs having an excellent cathode /anode impedance, high voltage is easily achieved and therefore limitations occur only from HV insulation problems or other technological reasons as e.g. power supply availability.

Also for HEMP-Ts high anode voltage can be adjusted and high specific impulse can be obtained due to its good axial electron impediment (see **1)**, above). But the limitations working for HEMP-Ts are occurring a little earlier than for GITs. Since a small portion of plume electrons (limited by the cusp mirror conditions) can directly pass near

the center through the exit, the released kinetic energy will heat the ceramic wall at that cusp and provide a thermal material depending limitation. This is typically achieved around 1200 V to 1500 V anode voltage.

For HETs the same argument is valid in principle. But since there the ceramic walls would not only be hit by higher energy electrons but also by more electrons, which in return lead to a higher ion current impact on this dielectric, the sputter effect would increase quadratic for higher anode voltage. Therefore life time limitations will prevent from long time high specific impulse operation of HETs. Typical operation voltages are 250V to 500V.

7) Power to thrust ratio (PTTR)

The PTTR is defined as $PTTR = P/T$ and again for an ideal fully single charged ion beam $PTTR = \frac{I \cdot U}{I \cdot \sqrt{2 \cdot (M/q) \cdot U}} = \sqrt{\frac{q \cdot U}{2 \cdot M}}$, which is except the factor 2g for this case the same as the Isp, but is measured in W/mN. P is the anode power I and U are anode current and voltage, respectively.

Depending on the system requirements (e.g. low solar power available) it could be a goal to keep the PTTR rather low. In such case the HETs have an advantage because they can work efficiently at low voltage.

For HEMP-Ts low voltage operation is in principle possible, but the thrusters are designed for relative small channel cross section. For constant power, lowering the voltage would increase the current and thus the Xe gas flow reciprocally. For higher gas flow the neutral gas pressure would increases in the channel. Also the plasma column diameter would increase, which would start to produce plasma losses at the channel walls and decrease the thruster efficiency. In future, larger diameter HEMP-Ts could overcome this difficulty and may allow effective operation down to 300V.

For GITs low voltage is a technological hurdle because at a given power level the anode current should increase reciprocally which can not be obtained by increasing the gas flow because it would be in contradiction with the space charge limitation given by the Child-Langmuir law $I \sim U^{3/2}$. That means, higher current could only be obtained by a different thruster with either increased thruster area or a higher perveance grid structure with a reduced grid distance, which has mechanical tolerance limitations.

The following compared characteristics have a strong influence on the EP system requirements as electronics and control software:

8) Turn on/off characteristics (neutraliser operating)

HEMP-T: Assuming the neutraliser operating and providing electrons the thruster exit, there are only two further conditions to operate the HEMP-T. One is a neutral gas flow through the thruster and the other is an applied anode voltage sustaining the discharge power. The achieved operational status is independent of the sequence both supplies are turned on or off. Therefore two natural sequences are offered.

a) Gas first: Depending on the power supply characteristics, the discharge operates light bulb like within 20 to 100 milliseconds after anode power supply turn on and close to its nominal conditions (except small thermal drifts).

b) Voltage first: Depending on the plenum effect of the Xe feed line (diameter & length to valve), the thruster ignites at very low gas flow levels, operates with increasing thrust levels until it reaches its nominal conditions within few seconds (again except the thermal drifts). This very unique turn on and off mode is based on the very high impedance between cathode and anode when no gas is fed into the thruster (no electron collision partners are available to cross the cusp magnetic fields). Since it allows a very simple EP-system architecture as it replaces thruster switching units when operating several thrusters on a common anode line and since it can be used for throttling and thrust vectoring over a wide dynamic range, it is the proposed turn on/off and control process for HEMP-T based EP-systems (see papers[1,4,7] in these proceedings).

HET: Since HETs are not using permanent magnets but discharge current fed solenoids, a high gas discharge peak of neutraliser and thruster together is required to ignite both devices at the same time. Since there is some randomness in the ignition an automatic series of turn on trials has to be electronically controlled. Also a slow adjustment procedure of the anode voltage to the final operating point is required to avoid instable intermediate operation modes. The turn on process requests additional circuits and control loops on PSCU side.

GIT: Due to the different type of ionization processes, the ignition processes are both complex but quite different for RITs and EITs. Both start with the neutraliser first in operation and the acceleration grid polarized negatively.

- The RITs then turn on the RF generator to provide the ionization power. Discharge is ignited by providing a short positive voltage pulse to the acceleration grid in order to have a sufficient amount of electrons in the discharge chamber to start the steady ionization. During this ignition process the plasma conditions and thus the Rf-impedance changes which needs some readjustments on the RF generator circuits until steady operation conditions are obtained.
- For the EITs the next step is to start the main thermionic hollow cathode by preheating and igniting the main cathode with a keeper voltage pulse. After that, the heater has to be switched off and the keeper current to be adjusted to its steady state value when the main cathode to anode discharge current is adjusted. As a last step, the anode to EP ground voltage has to be turned on which in turn switches the ion beam on.

Both thruster type procedures require a lot electronic control circuits and respective software.

9) Continuous operation

In discharge plasmas a lot of instabilities can occur, which lead to respective oscillations. GITs are considered to be the most stable thrusters in this respect (lowest ac content in discharge anode current). But they are suffering from erratic discharge events between the grids which lead to so called flame out events, requiring automatic restart electronics.

The dominating contributions at the lowest frequencies, typically stem from the ionization front phenomena, where ionization moves towards the neutral gas inlet, leaving behind this movement a neutral atom exhausted volume, reducing the discharge current significantly until this volume is refilled and the cycle restarts again. This effect depends strongly on the geometrical distribution of the gas inlet(s) and eventual magnetic field configurations.

For HEMP-Ts this thruster oscillation is rather periodic in the 100 kHz range with an ac amplitude modulation of about 30% of the average discharge current. Both, amplitude and frequency have only little dependence on anode voltage and gas flow. Typical examples are mentioned in[4]. Above 500 kHz no discrete spurious where noticed so far up to 20 MHz in the conducted emission on the anode line. Further radiated emission tests need to be performed.

For HETs it is known that a periodic oscillation regime is limited to certain operation modes relating anode voltage and discharge current to limited ratio bands. In this best case the oscillation frequency is around 20 kHz and the amplitude modulations can vary widely and can go up to 100%. A lot of literature is available on this topic and some presented on this conference. In many cases in addition to the base frequency a lot of other instabilities occur, which make the discharge current noisy.

10) Life limiting erosion effects

In contrast to the well examined GITs and HETs, the least information is available for the HEMP-Ts, simply due to the lack of life test and in orbit experience. It is planned to perform a multiyear ground life test within the IOD (in orbit demonstration) program of the HEMP-Ts for SGEO between 2008 and 2011 which will close this gap. A 250h endurance test at 57 mN and 1.8 kW was performed on HEMP-T DM7, followed by a destructive physical analysis of the discharge channel. This indicated its capability for a minimum total impulse of 3.8 MNs (corresponding to 18 years continuous life)[8,9,10]. A potential minor life impact could remain from plume and charge exchange ions, which are accelerated back to the grounded thruster structure. Meanwhile the longest controlled operation time was 900 h in two subsequent each 450 h tests with HEMP-T DM 9.1, which confirmed the earlier findings.

Since the total impulse depends on the thruster size and thrust level, it is difficult to perform a direct comparison with other thruster types. The life expectation of the 250 mN, 7.5 kW HEMP-T 30250 is expected by scaling laws to range > 20 MNs for the total impulse.

11) PSCU requirements and auxiliary supplies (AS)

In the para 8) above we have already pointed out the physical reasons for the simple architecture of a HEMP-T PSCU in comparison to the HET - and GIT PSCUs. Here we refer to item 11 of the following table 2.1, which summarizes these aspects. From there it is obvious that the simplicity of the HEMP-T PSCU will be a major source for the cost competitiveness of a HEMP-T EP system.

12) Several thrusters operating on one anode line

Within the ESA TRP Study *High power HEMP thruster module*, it could be verified that two thrusters can operate on one anode voltage supply line completely independent with respect to their thrust level and turn on/off situation. In the previous items above the physical reasons were explained. As long as these physical conditions do not apply to the other thruster concepts, it is assumed that this parallel but independent operation is not possible.

Table 2.1 Summary of the physical and operational comparison between thruster types
The physically best suited characteristic for each item is highlighted by **bold** typing.

No	Property	HEMP-T	HET	GIT	HEMP-T like
1)	**Axial electron impediment by:**	magnetic multi-cusps	extended radial B-field zone	**negative polarized acceleration grid**	HET
2)	**Ion beam power efficiency**	**high**	low	**high**	GIT
3)	**Operation capability without neutraliser**	**yes**	no	**yes**	GIT
4)	**Plasma confinement in discharge chamber**	**yes, magnetically, almost complete in multiple magnetic cells**	low level magnetically but wall contact is required to sustain the discharge	RIT: no confinement EIT: yes, magnetically	unique
5)	**Separation of ionization and acceleration zones**	yes, magnetically separated by exit cusp	no, ionization and acceleration are overlapping	**yes, separated by screen grids**	GIT
6)	**Specific impulse/s**	adjustable medium range 2000-3500	adjustable low range 1000 to 2000	**adjustable high range 3000 to >5000**	GIT
7)	**Power to thrust ratio / W/mN**	medium, adjustable 20 to 35	**low, adjustable 15 to 20**	high, adjustable 30 to 40	HET
8)	**Turn on/off characteristics**	**very simple,** 2 modes possible: - Xe first: light bulb like operation with Ua on/off in ms - Ua first: soft turn on/off in s with gas flow turned on/off	complex, simultaneous ignition of neutraliser and thruster (solenoids for magnet fields are fed by discharge anode current)	complex, RIT: Ignition with short positive polarization on ac-celleration grid allows neutraliser electrons to ignite RF discharge. EIT: Ignition of main cathode to ignite discharge	unique
9)	**Continuous operation**	**very stable periodic osillations ~100kHz**	noisy, with base frequency ~ 20 kHz	mainly dc, but erratic flame outs by shorts, discharges between grids	unique
10)	**Life limiting erosion effects**	**minimal on low potential exit structure by charge exchange ions**	Yes, discharge chamber walls by direct impact and exit structure by charge exchange ions	Yes, acceleration grid by direct impact and returned charge exchange ions	unique
11)	**PSCU requirements,**	**very simple**	Simple	RIT: complex EIT: very complex	unique

	Auxiliary supplies and equipment except anode and 1 neutraliser	**no auxiliary supplies, due to permanent magnets plasma confinement.**	2nd neutraliser + solenoid supply, + filter unit + thruster switching unit	acceleration grid supply + thruster switching unit + for RIT: RF generator EIT: main cathode, + solenoids	unique
12)	**Several thrusters operating on 1 anode line**	**yes, gas flow used to control and turn on off**	no, only sequential operation with TSU	no, only sequential operation with TSU	unique

III. Simplified Power Balance Model of the HEMP-Thruster

Throughout the hardware development phase, the Thales EP team tried to use an available particle in cell code to support their optimisation steps. A suited code, recommended by the IOM team in Leipzig, was the XOOPIC code developed by the Berkeley University team around Birdsall. Even without training on the code and without numerical expertise, some few questions are believed to be solved with XOOPIC. Examples are the identification of the ionization zones close to the thruster axis, slightly downstream the center cusp and the anode cusp (compare figure 3.1) and the charging of the ceramic wall during the thruster ignition. Though including first order collissional processes in their Monte Carlo package, as single stage ionization and elastic electron scattering, important second order effects, as double ionization, charge exchange reactions and neutral background gas particle injection, are not included in the XOOPIC code, preventing selfconsistant solutions. Another, deeper code problem not solved by our team, was the violation of energy conservation between succeeding time steps leading to collective almost exponentially increasing plasma oscillations and particle numbers. These problems were likely magnified by our too coarse mesh sizes and too high particle densities in the HEMP-T magnetic plasma confinement. As a consequence, it was not possible to provide valid plasma potential distributions inside the multi stage discharge channel from those simulations. Also experimental probe measurements so far were not successful, because probing on the axis directly interrupts the path with highest current densities and disturbs significantly the plasma discharge. Therefore we tried to find with a simplified power balance model a method to determine the plasma potential distribution along the thruster axis for the different magnetic cells and to confirm the visually expected steep drop at the thruster exit cusp. The one-dimensional energetic model proposed here, was quite successful in that respect.

A. The simplified HEMP-T model

The model is sketched out in figure 3.1.* Following assumptions are specifying it:

1. Three magnet rings define four plasma cells, separated by three neutral- or cusp flux lines, indicated in figure 3.1 as dotted lines. Within each plasma cell, the potentials are considered constant and have to be selfconsistantly determined: $\phi 1$ in front of the exit cusp, $\phi 2$ between exit cusp and center cusp, $\phi 3$ between center cusp and anode cusp and $\phi 4$ between anode cusp and anode.

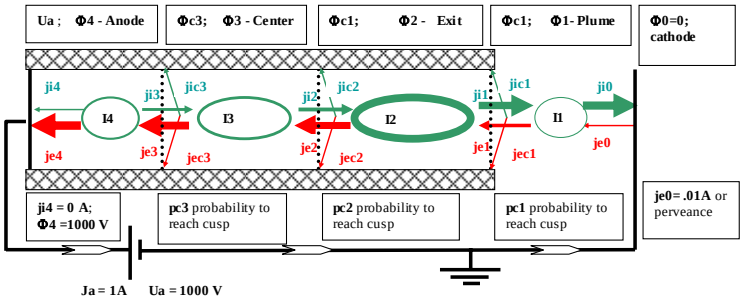

Fig 3.1 Simplified circuit and power balance model of the HEMP-Thruster

* Figure 3.1 shows nicely the similarity of the HEMP-T with a multistage grid ion engine. The neutral cusp flux lines can be interpreted as magnetic 1- hole grids.

2. Upstream of each cell, electrons can hit at the cusps the dielectric material of the channel wall which requests an identical ion current for charge compensation. This condition determines selfconsistantly adjusting cusp potentials $\phi c1$, $\phi c2$, $\phi c3$.
3. The potential boundary conditions are at the cathode $\phi 0 = 0V$ and at the anode Ua = 1000 V to simulate a typical operating condition.
4. The current boundary condition at the anode has been set to Ja=1A, since no ionization cross sections and no neutral gas flow assumptions are made in this model. At the cathode we assume for simplicity a space charge limited cathode emission described by a selected perveance p0 ($je0=p0 \cdot U^{3/2}$).
5. At each cusp the sum of electron and ion current should be 0 due to the dielectric boundary condition.
6. For each magnetic cell the charge conservation is valid, that means the sum of entering and leaving currents has to be zero.
7. For each magnetic cell the energy conservation is valid by requiring that the entering kinetic electron power is equal to the ionization-, thermalisation-, excitation losses and the dissipated power losses occurring by direct electron current impact at the respective cusp. For the cusp losses, we assume that only slow ions from its respective magnetic cell can hit the ceramic wall at its cusp, which means that no accelerated ions from a more upstream magnetic cusps hits downstream the ceramic wall (this is in agreement with the experimental experience).
8. Ionization and excitation losses are considered as frozen losses not contributing to the thermal load of the thruster, except the recombination losses at boundaries.
9. The ionization produces equal amounts of electron and ion source current terms I1 to I4.
10. Thermalisation power (unordered kinetic power) is distributed as temperature to the thermalised electrons and transported by collisions to the next upstream magnetic cell (finally to the anode) or according to the magnetic mirror conditions to the respective cusp as dissipated loss.
11. The material properties of e.g. Xe are included in the relative ratios Ci, Ce and Ct to which the entering power of electrons within the magnetic cusp mirror condition is distributed to ionization, excitation and thermalisation. In the model they are selected to match the observed thermal losses of about 15%. Also the ionization energy is assumed with 12.1 eV.
12. Finally the overall power conservation requests that the delivered electric power $Ua \cdot Ia$ has to equal the ion beam power Pb, the frozen losses and all thermal dissipations at anode and the respective magnetic cusps.

B. The simplified equation system

With the specifications provided above we can formulate an equation system with 28 equations for the 28 unknown parameters:

- **4** plasma potentials $\phi 1$ to $\phi 4$,
- **3** cusp potentials $\phi c1$ to $\phi c3$ at the ceramic surface,
- **4** electron temperatures T1 to T4,
- **4** ionization source currents I1 to I4 in the plasma cells,
- **5** electron currents je0 to je4,
- **5** ion currents ji0 to ji4,
- **3** ion cusp currents jic1 to jic3.

Global power balance equation (1):

electric power $Ua \cdot Ja$ = Beam power Pb + Ionization losses IL + Excitation losses EL + Cusp losses CL (electronic-, ionic- and recombination) + anode losses AL (electronic- ionic and recombination), with:

$$Pb = (ji3) \cdot \Phi 4 + (ji2 - ji3) \cdot \Phi 3 + (ji1 - ji2) \cdot \Phi 2 + (ji0 - ji1) \cdot \Phi 1$$

$$IL = IE \cdot (I1 + I2 + I3 + I4)$$ where IE= 12.1 eV, Xe Ionization energy, Im : Ionization source currents, tbd.

$$EL = CEje0(1 - p1) \cdot \Phi 1 + CEje1 \cdot (1 - p2) \cdot (\Phi 2 - \Phi 1 + T1) + CEje2 \cdot (1 - p3) \cdot (\Phi 3 - \Phi 2 + T2) + CEje3(1 - p4) \cdot (\Phi 4 - \Phi 3 + T3)$$

where CE is the relative proportion of the gained electron power transferred to excitation. Here CE=0.25, CI= 0.07 the proportion for ionization and for thermalisation CT= 0.68 (CE+CI+CT=1) are selected. The pm-values are the probabilities of electrons to reach the dielectric wall and to be not reflected by the cusp mirror condition, see section II, 4) above.

CL=

$$je0 \cdot p1 \cdot (\Phi c1 - \Phi 0 + \Phi 1 - \Phi c1 + IE) + je1 \cdot p2 \cdot (\Phi c2 - \Phi 1 + \Phi 2 - \Phi c2 + IE + T1) + je2 \cdot p3 \cdot (\Phi c3 - \Phi 2 + \Phi 3 - \Phi c3 + IE + T2)$$

AL = $je3 \cdot p4 \cdot (Ua - \Phi 3 + T3) + (I4 + je3 \cdot (1 - p4)) \cdot (\Phi 4 - Ua + T4) - ji4 \cdot (\Phi 4 - Ua)$

CL and AL are the cusp - and anode losses, respectively.

Power balance equations for each magnetic cell (4):
Received electron power from downstream cell = direct cusp loss + thermalised power + ionization loss + excitation loss:

$$je0 \cdot (1 - p1) \cdot (\Phi 1 - \Phi 0 + T0) + je0 \cdot p1 \cdot (\Phi c1 - \Phi 0 + T0) = je0 \cdot p1 \cdot (\Phi c1 - \Phi 0 + T0) + (je0 \cdot (1 - p1) + I1) \cdot T1 + I1 \cdot IE + je0 \cdot (1 - p1) \cdot CE \cdot (\Phi 1 - \Phi 0 + T0)$$

$$je1 \cdot (1 - p2) \cdot (\Phi 2 - \Phi 1 + T1) + je1 \cdot p2 \cdot (\Phi c2 - \Phi 1 + T1) = je1 \cdot p2 \cdot (\Phi c2 - \Phi 1 + T1) + (je1 \cdot (1 - p2) + I2) \cdot T2 + I2 \cdot IE + je1 \cdot (1 - p2) \cdot CE \cdot (\Phi 2 - \Phi 1 + T1)$$

$$je2 \cdot (1 - p3) \cdot (\Phi 3 - \Phi 2 + T2) + je2 \cdot p3 \cdot (\Phi c3 - \Phi 2 + T2) = je2 \cdot p3 \cdot (\Phi c3 - \Phi 2 + T2) + (je2 \cdot (1 - p3) + I3) \cdot T3 + I3 \cdot IE + je2 \cdot (1 - p3) \cdot CE \cdot (\Phi 3 - \Phi 2 + T2)$$

$$je3 \cdot (1 - p4) \cdot (\Phi 4 - \Phi 3 + T3) + je3 \cdot p4 \cdot (\Phi c4 - \Phi 3 + T3) = je3 \cdot p4 \cdot (\Phi c4 - \Phi 3 + T3) + (je3 \cdot (1 - p4) + I4) \cdot T4 + I4 \cdot IE + je3 \cdot (1 - p4) \cdot CE \cdot (\Phi 4 - \Phi 3 + T3)$$

Current balances or boundary interface conditions (8):

$Ja = je4 + ji4 \quad Ja = je3 + ji3 \quad Ja = je2 + ji2 \quad Ja = je1 + ji1 \quad Ja = je0 + ji0$ constant current at 3 Interfaces and 2 Electrodes

$je0 \cdot p1 = jic1 \quad je1 \cdot p2 = jic2 \quad je2 \cdot p3 = jic3$ zero currents at 3 dielectric cusps

Definition equations (15):

$$je0 = p0 \cdot \Phi 1^{\frac{3}{2}} \qquad I1 = je0 \cdot (1 - p1) \cdot CI \cdot \left(\frac{\Phi 1 - \Phi 0 + T0}{IE} \right) \qquad ji0 = ji1 + I1 - jic1$$

$$je1 = je0 \cdot (1 - p1) + I1 \qquad I2 = je1 \cdot (1 - p2) \cdot CI \cdot \left(\frac{\Phi 2 - \Phi 1 + T1}{IE} \right) \qquad ji1 = ji2 + I2 - jic2 \qquad T2 = \frac{CT \cdot je1 \cdot (1 - p2) \cdot (\Phi 2 - \Phi 1 + T1)}{je2}$$

$$je2 = je1 \cdot (1 - p2) + I2 \qquad I3 = je2 \cdot (1 - p3) \cdot CI \cdot \left(\frac{\Phi 3 - \Phi 2 + T2}{IE} \right) \qquad ji2 = ji3 + I3 - jic3 \qquad T3 = \frac{CT \cdot je2 \cdot (1 - p3) \cdot (\Phi 3 - \Phi 2 + T2)}{je3}$$

$$je3 = je2 \cdot (1 - p3) + I3 \qquad I4 = je3 \cdot (1 - p4) \cdot CI \cdot \left(\frac{\Phi 4 - \Phi 3 + T3}{IE} \right) \qquad ji3 = I4 - |ji4| \qquad T4 = \frac{CT \cdot je3 \cdot (1 - p4) \cdot (\Phi 4 - \Phi 3 + T3)}{je3 \cdot (1 - p4) + I4}$$

Additional solution restrictions:
In addition to these equations, we need to define plausible physical restrictions for the allowed solution:

$T1 > 0 \quad T2 > 0 \quad T3 > 0 \quad T4 > 0 \quad \Phi c1 < \Phi 1 \quad \Phi c2 < \Phi 2 \quad \Phi c3 < \Phi 3 \quad |ji3| > |ji4|$

$0 < \Phi 1 \quad \Phi 1 < \Phi 2 \quad \Phi 2 < \Phi 3 \quad \Phi 3 < \Phi 4 \quad \Phi 4 > 1000 \quad 0 < \Phi c1 \quad \Phi c1 < \Phi c2 \quad \Phi c2 < \Phi c3 \quad ji4 < 0$

Due to the opposite direction of ji4 to the anode, this current must be negative, the other restrictions are mainly self-explaining,.

C. Solution of the simplified HEMP-T models

To solve this equation system the "*MathCAD 8 professional"* code in its German version was used. Two solvers are available. The first solver "*suchen"* did mostly not work for the 28 equation problem. Therefore the "*minfehl"* command was used seeking for solution with minimum failure. The power accuracy of the solution was in this case always within 0.5%. Solutions were found for the standard 3 cusps, 4 cells HEMP-T DM9.2 and for a new development HEMP-T DM10, which is in assembly but at the time of writing not yet tested. Both models are compared with even simpler thrusters with only 1 cusp, (2 magnetic cells). For those reduced models (14 equations, 14 unknown), the "*suchen*" command was always successful. In this case the power failure was less than 0.1 %. Except the lower number of magnetic stages, the two cell thrusters are calculated with the same electric and magnetic boundary conditions where applicable. The cross comparison of the 4 models provides interesting views on the HEMP-T physics as we will see from a review of table 3.1.

Table 3.1. Solution of the simplified power balance models of HEMP-T thrusters with Ua=1kV anode voltage and Ja=1 A anode current (boundary conditions)

Parameter/ Type	DM 9.2; 4 stage	DM 9.2; 2 stage ref.	DM 10; 4stage	DM10 2 stage ref.	Remarks
Φ1/ V	14.1	18.4	12.3	17.4	plume potential
Φ2/ V	1000	1010	979	1005	exit cell potential
Φ3/ V	1000	-	999	-	center cell potent.
Φ4/ V	1000	-	1000	-	anode cell potent.
Φc1/ V	8.1	8.1	12.2	7.6	exit cusp potent.
Φc2/ V	960	-	979	-	main cusp potent.
Φc3/ V	965	-	979	-	anode cusp potent
T1/ eV	8.9	11.3	7.8	10.8	plume el. temp.
T2/ eV	100.1	100.3	99.8	100.2	exit cell el. temp.
T3/ eV	43.1	-	48.1	-	center cell temp.
T4/ eV	23.5	-	26.2	-	anode cell temp.
I1/ A	0.008	0.016	0.006	0.014	plume source curr.
I2/ A	0.543	0.836	0.473	0.844	exit source curr.
I3/ A	0.310	-	0.361	-	center source curr.
I4/ A	0.157	-	0.229	-	anode source curr.
je0/ A	0.106	0.158	0.086	0.145	cath. emission
je1/ A	0.107	0.164	0.090	0.156	up exit cusp
je2/ A	0.637	1.000	0.557	1.000	up main cusp

Parameter/ Type	DM 9.2; 4 stage	DM 9.2; 2 stage ref.	DM 10; 4stage	DM10 2 stage ref.	Remarks
je3/ A	0.845	-	0.882	-	up anode cusp
je4/ A	1.002	-	1.111	-	to anode
ji0/ A	0.894	0.842	0.914	0.855	ion beam
ji1/ A	0.893	0.836	0.910	0.844	down exit cusp
ji2/ A	0.363	-0.000	0.442	-0.000	down center cusp
ji3 A	0.155	-	0.118	-	down anode cusp
ji4/ A	-0.002	-	-0.111	-	to anode
jic1/A	0.007	0.010	0.002	0.004	to exit cusp
jic2/A	0.013	-	0.006	-	to main cusp
jic3/A	0.102	-	0.037	-	to anode cusp
Pbeam/ W	891.6	844.5	899.4	848.3	kinetic power
IonisationLoss/ W	12.3	10.3	12.1	10.4	sum all sources
Anode Loss/ W	27.7	108.2	31.0	104.2	sum electr. + ions
Cusp Loss/ W	22.9	0.3	10.0	0.15	sum electr. + ions
ExcitationLoss/ W	51.43	36.8	51.43	37.1	frozen+ radiated
Beam efficiency%	89.16	84.45	89.94	84.8	electric—>kinetic
Ionization Cost /V	121.5	184.7	110.1	177.5	IC=(Ua*Ia-Pbeam)/ji0
CI+CE+CT=1	0.07+0.25+0.68	0.07+0.25+0.68	0.07+0.25+0.68	0.07+0.25+0.68	assumed only
Perveance p0	0.002	0.002	0.002	0.002	$ie0=p0\cdot\Phi 1^{3/2}$
Cusp arr. prob. p1	0.06	0.06	0.024	0.024	magnetic circuit
Cusp arr. prob. p2	0.119	0.119	0.064	0.064	magnetic circuit
Cusp arr. prob. p3	0.160	-	0.066	-	magnetic circuit
Cusp arr. prob. p4	0.254	-	0.092	-	magnetic circuit

Conclusions:

The detailed figures of table 3.1 should be considered only as very rough indicators, because essential physical characteristics and phenomena of the thrusters are not considered in the model. Those are for instance, without claiming for completeness: neutral gas density distribution, ionization efficiency and specific impulse, double ionization of Xe, a realistic electron velocity distribution rather than global temperatures in each cell, the angular distribution of the ion beam, etc.. All these important effects could only be treated with a particle in cell code, which is not (yet) available on the market. Nevertheless the simple model is by definition a stationary solution approach, indicating the average characteristics of the thruster. Following major observations can be highlighted:

1. Potentials: The large potential drop occurs as expected between the plume and the exit cell at the exit cusp. The potential differences between stage 2, 3 and 4 are rather small. However, as we note from the next point, the higher number of magnetic cusps and cells have a very positive effect on the electron temperatures in the anode cell and efficiency.
2. Temperatures: typically the electron temperatures are around 100eV in the exit cell. This enormous kinetic energy content is used positively in the next upstream cells for ionization. Therefore the temperature is reduced in the anode cell for the 4 cell thrusters down to about 25 eV, which increases the efficiency.
3. Efficiency: Due to the better electron cooling at the anode level, the 4 cell thrusters have about 5% higher beam power efficiency then the 2 cell thrusters. There, all the fast electrons impinge directly on the anode, leading to 3 times the anode losses of the 4 cell thrusters. The better electron confinement in DM10 is predicted to lead to only less than 1% better beam efficiency but has very positive effects on the cusp losses.
4. Cusp losses: The exit cusp is due to its low current levels almost without losses. Therefore a one cusp thruster has almost no cusp losses at all. The two 4 cell thrusters differ significantly in their cusp losses. The better magnetic confinement of the DM10 thruster promises only 50% of the cusp losses compared to DM9.2. This would be a major technological improvement, because the thermal load on the thin ceramic wall determines one of the power limitations of the HEMP-T concept. This improved confinement is also indicated by the much lower cusp arrival probabilities p1 to p4 for the DM10 thruster type.
5. No cusp erosion: The observed lack of ion erosion at the cusps is supported a) by the low cusp ion currents and b) the small voltage difference between cusp potential and its respective plasma potential in the order of 20 (DM10) to 40 V (DM9.2) depending on the different plasma confinement properties.
6. Excitation losses: As can be expected, the excitation losses for single cusp thrusters are lower then for the triple cusp thrusters. We find about 37 W compared to 51 W, respectively.
7. Only a small difference can be seen in the frozen ionization losses, which takes with about 12 W for the 4 cell thrusters and about 10 W for the 2 cell versions only 1.2% and 1%, respectively of the electric power delivered to the thrusters. The difference itself is caused by the differences in the source terms.
8. Ionization costs: due to the lower beam power of the 2 cell thrusters, the ionization costs are with 180 V significantly higher than the 110 V ionization costs of the 4 cell thrusters, again justifying the multistage HEMP-T concept.

In summary, the presented simplified power balance model appears as tool, connecting the thruster's magnetic circuit properties with its global plasma characteristics by using the cusp mirror laws of plasma electron confinement in strong magnetic field gradients. This allows predictions on beam power efficiency and the thruster loss terms as well as estimations on internal plasma potentials and electron temperatures which are quite important from the thruster's technological point of view. Since ionization and angular efficiencies are not covered, prediction of the total thruster efficiency is not possible. For the future, it might be interesting to replace the ratios CI, CE and CT, chosen to adapt the model to the observed thermal properties of the thruster, by independently measured values.

Acknowledgments

The authors would like to express their thanks for the steady support of the agencies to the development of the HEMP-T concept. Here the German Aerospace Center DLR must be mentioned at first position and here especially Ralf Dittmann, Hans Meusemann and recently Gerd Kraft and Norbert Püttmann. They all contributed with their support to our progress in the hardware development and the understanding. Very positive impulses were received in

the first difficult years by the French CNES, mainly from Ann Cadiou and Franck Darnon. Encouragement over long periods was observed from the European Space Agency ESA, resulting in a running TRP program for the development of a high power HEMP-T module. This has to be thanked to Giorgio Saccoccia, José Gonzales del Amo, Denis Estublier and Eric Gengembre. Recently, a lot of support was experienced also by the ESA ARTES11 SGEO project team lead by Antonio Garutti. Since it would take too much space to mention all the individuals helping us within the companies of our industrial and institutional partners, we acknowledge them by mentioning their company's names as Astrium in Friedrichshafen and in Toulouse, IOM-Leipzig, IPP Greifswald, OHB and Thales Alenia Space in Cannes and in Charleroi.

For a series of fruitful discussions fostering his physical understanding of the plasma processes, the first author wants to thank especially Werner Schwertfeger in Ulm, Prof. Bouchoule in Orleans, Jean Bonnet and Prof. Rax in Palaiseau.

References

1. H. Lübberstedt, Th. Miesner, A. Winkler, P. Rathsman, J. Kugelberg, "Solely EP based Orbit Control System on Small GEO Satellite", *Proceedings of the 30th International Electric Propulsion Conference,* Florence 2007, IEPC-2007-274
2. H.-P. Harmann, N. Koch, G. Kornfeld: "Low Complexity and Low Cost Electric Propulsion System for Telecom Satellites Based on HEMP Thruster Assembly", 30th International Electric Propulsion Conference, Florence Sep. 2007, Paper 114.
3. G.Kornfeld, N.Koch, G. Coustou, "First Test Results of the HEMP Thruster Concept", proceedings of the 28th International Electric propulsion Conference, Toulouse, 2003, IEPC 2003-112.
4. H.-P. Harmann, N. Koch, G. Kornfeld: "The ULAN Test Station and its Diagnostic Package for Thruster Characterization", 30th International Electric Propulsion Conference, Florence Sep. 2007, Paper 119.
5. N. Koch, H.-P. Harmann, G. Kornfeld: "Status of the THALES High Efficiency Multi Stage Plasma Thruster Development for HEMP-T 3050 and HEMP-T 30250", 30th International Electric Propulsion Conference, Florence Sep. 2007, Paper 110.
6. N. Koch, G. Kornfeld, H.-P. Harmann: "Status of the THALES Tungsten/Osmium Mixed-Metal Hollow Cathode Neutralizer Development", 30th International Electric Propulsion Conference, Florence Sep. 2007, Paper 117
7. M. Gollor, M. Boss, F. Herty and B. Kiewe " Generic High Voltage Power Supplies (HVPS) with Optimum Efficiency and Multi-Range " Proceedings 30th International Electric Propulsion Conference, Florence, Italy, 17.-20th Sept. 2007, No. 21
8. G. Kornfeld, N. Koch, H. P. Harmann; New Performance and Reliability Results of the Thales HEMP Thruster; Proceedings of the 4th ISPC; Cagliari, 2004.
9. N. Koch, H.-P Harmann and G. Kornfeld, "Development and Test of the THALES High Efficiency Multistage Plasma (HEMP) Thruster Family" Proceedings of the 29th International Electric Propulsion Conference, Princeton University, October 31 – November 4, 2005 - IEPC-2005-297
10. G. Kornfeld, N. Koch, H.-P. Harmann, P. Micheli, H. Meusemann, E. Gengembre: „High Power HEMP-Thruster Module, Status and Results of a DLR and ESA Development Program", 42nd AIAA/ASME/SAE/ASEE Joint Propulsion Conference & Exhibit, Sacramento, California, July 2006, Paper AIAA 2006- 60150